FDG-PET studies performed under baseline conditions (*6*). The question remaining is which is the best indicator of regional brain function. In our subject, for example, the significant difference observed in the absolute measures between studies 1 and 2 was lost for the relative measures. One could question whether the differences observed with the absolute measures represent noise or whether the relative measures are less sensitive to physiological signals. This issue is important since increasing numbers of imaging studies that evaluate functional activation use relative rather than absolute measures. Relative measures assume that regional measures change linearly with respect to changes in global metabolism and/or global cerebral blood flow. Studies are required to establish the relationship between the changes in metabolic activity in the various brain regions as a function of changes in whole brain metabolism.

CONCLUSION

Regional brain metabolic changes induced by the benzodiazepine agonist are highly reproducible in magnitude and pattern. We found that also shows that the metabolic rate was consistently lower in the second study than in the first. The mechanism accounting for the decreases in the replication study requires further evaluation.

ACKNOWLEDGMENTS

We thank D. Alexoff, C. Barrette, R. Carciello, T. Johnson, P. King, A. Levy, T. Martin, R. MacGregor, N. Netusil, C. Redvanly, D. Schlyer, C. Shea, D. Warner and C. Wong for their participation in various aspects of this work. This work was supported by the U.S. Department of Energy under Contract DE-ACO2-76CH00016 and NIAAA grant 1RO1 AA09481-01.

REFERENCES

1. Volkow ND, Fowler JS. Neuropsychiatric disorders: Investigation of schizophrenia and substance abuse. *Semin Nucl Med* 1992;12:254–267.
2. Volkow ND, Wang G-J, Hitzemann RJ, et al. Recovery of brain glucose metabolism in detoxified alcoholics. *Am J Psych* 1994;151:178–183.
3. Mazziotta JC, Phelps ME. Positron emission tomography studies of the brain. In: Phelps ME, Mazziotta J, Schelbert H, eds. *Positron emission tomography and autoradiography.* New York: Raven Press; 1986:493–579.
4. Sokoloff L. Measurement of local cerebral glucose utilization and its relation to local functional activity in brain. In: Vranic M, Efendic S, Hollenberg CH, eds. *Fuel homeostasis and the nervous system.* New York: Plenum Press; 1991:21–42.
5. Duara R, Gross-Glenn K, Barker WW, et al. Behavioral activation and the variability of cerebral glucose metabolic measurements. *J Cereb Blood Flow Metab* 1987;7:266–271.
6. Bartlett EJ, Brodie JD, Wolf AP, Christman DR, Laska E, Meissner M. Reproducibility of cerebral glucose metabolic measurements in resting human subjects. *J Cereb Blood Flow Metab* 1988;8:502–512.
7. Volkow ND, Hitzemann RJ, Wolf AP, et al. Acute effects of ethanol on regional brain glucose metabolism and transport. *Psych Res* 1990;35:30–48.
8. Buchsbaum M, Wu J, Haier R, et al. Positron emission tomography, assessment of effects of benzodiazepines on regional glucose metabolic rate in patients with anxiety disorder. *Life Sci* 1987;40:2393–2400.
9. Morrow AL, Paul SM. Benzodiazepine enhancement of g aminobutyric acid-mediated chloride ion flux in rat brain synaptoneurosomes. *J Neurochem* 1988;50:302–306.
10. De Wit H, Metz J, Wagner N, Cooper M. Effects of diazepam on cerebral metabolism and mood in normal volunteers. *Neuropsychopharmacology* 1991;5:33–41.
11. Volkow ND, Wang G-J, Hitzemann RJ, et al. Decreased cerebral response to inhibitory neurotransmission in alcoholics. *Am J Psych* 1993;150:417–422.
12. Brogden RN, Goa KL. Flumazenil: a preliminary review of its benzodiazepine antagonist properties, intrinsic activity and therapeutic use. *Drugs* 1988;35:448–467.
13. Volkow ND, Wang G-J, Begleiter H, et al. Regional brain metabolic response to lorazepam in subjects at risk for alcoholism. *Alcohol Clin Exp Res* 1995;19:510–516.
14. Wang G-J, Volkow ND, Wolf AP, Brodie JD, Hitzemann RJ. Intersubject variability of brain glucose metabolism in young normal males. *J Nucl Med* 1994;35:1457–1466.
15. Woods JH, Katz JL, Winger G. Benzodiazepines: use, abuse and consequences. *Pharmacol Rev* 1992;44:154–347.
16. Wang G-J, Volkow ND, Roque C, et al. Functional importance of ventricular enlargement and cortical atrophy in healthy subjects and alcoholics as assessed by PET, MR imaging and neuropsychological testing. *Radiology* 1993;186:59–65.
17. Haggard EA. *Intraclass correlation and the analysis of variance.* New York: Dryden Press; 1958.
18. Winer, BJ. *Statistical principles in experimental design.* New York: McGraw-Hill 1972:217–280.
19. Volkow ND, Wang G-J, Hitzemann RJ, et al. Depression of thalamic metabolism by lorazepam is associated with sleepiness. *Neuropsychopharmacology* 1995;12:123–132.
20. Wieland HA, Luddens H, Seeburg PH. Molecular determinants in $GABA_A$/BZ receptors subtypes. In: Biggio G, Concas A, Costa E, eds. *GABAergic synaptic transmission: molecular, pharmacological and clinical aspects.* New York: Raven Press; 1992:29–40.
21. Foster NL, VanDerSpek AFL, Aldrich MS, et al. The effect of diazepam sedation on cerebral glucose metabolism in Alzheimer's disease as measured using positron emission tomography. *J Cereb Blood Flow Metab* 1987;7:415–420.
22. Gur RC, Gur RE, Resnick SM, Skolnick BE, Alavi A, Reivich M. The effect of anxiety on cortical cerebral blood flow and metabolism. *J Cereb Blood Flow Metab* 1987;7:173–177.
23. Henauer SA, Gallaher EJ, Hollister LE. Long-lasting single-dose tolerance to neurologic deficits induced by diazepam. *Psychopharmacology* 1984;82:161–163.

SPECT and MRI Evaluations of the Posterior Circulation in Moyamoya Disease

Ichiro Yamada, Yuji Murata, Isao Umehara, Soji Suzuki and Yoshiharu Matsushima

Departments of Radiology and Neurosurgery, Faculty of Medicine, Tokyo Medical and Dental University, Tokyo, Japan

We evaluated the posterior circulation in patients with moyamoya disease by SPECT and MRI. **Methods:** Six patients with idiopathic moyamoya disease were studied by SPECT, MRI and angiography. Patients received an injection of 555–740 MBq of ^{99m}Tc-HMPAO, after which SPECT images were taken. The cerebral-to-cerebellar activity ratio in five cerebral regions was calculated to assess the regional cerebral blood flow (rCBF). The SPECT and MRI findings were then compared with angiographic. **Results:** Of the 12 posterior cerebral arteries (PCAs) in the six patients studied, seven PCAs (58%) in five patients had a stenotic or occluded lesion. Furthermore, rCBF in all five regions significantly decreased as the degree of steno-occlusive lesions of the PCA progressed. No significant correlation, however, was found between the steno-occlusive lesions of the internal carotid artery bifurcation and the rCBF. The rCBF significantly decreased in the absence of leptomeningeal collateral vessels from the PCA to the anterior circulation. On the basis of the MR images, the frequency of cerebral infarctions significantly increased in patients with steno-occlusive PCA lesions. **Conclusion:** The rCBF in moyamoya disease decreases proportionally with the degree of steno-occlusive lesions of the PCA. The steno-occlusive PCA lesions decrease the number of leptomeningeal collateral vessels to the anterior circulation, thereby causing severe cerebral ischemia that is likely to result in infarctions.

Key Words: moyamoya disease; technetium-99m-HMPAO; regional cerebral blood flow; posterior circulation; SPECT

J Nucl Med 1996; 37:1613–1617

Received Oct. 6, 1995; revision accepted Jan. 24, 1996.

For correspondence or reprints contact: Ichiro Yamada, MD, Department of Radiology, Faculty of Medicine, Tokyo Medical and Dental University, 1-5-45 Yushima, Bunkyo-ku, Tokyo 113, Japan.

Although moyamoya disease, a rare cerebrovascular occlusive disease of unknown etiology, is commonly seen in Japan, cases have also been reported elsewhere (*1–4*). The angiographic features of this disease are as follows: (a) bilateral stenosis or occlusion of the supraclinoid portion of the internal carotid artery that extends to the proximal portions of the anterior cerebral artery and the middle cerebral artery and (b) the presence of parenchymal, leptomeningeal and transdural collateral vessels that supply the ischemic brain (*5–7*).

Recently, SPECT has been used to evaluate cerebral blood flow (CBF) in patients with moyamoya disease (*8–11*). Only a few reports, however, have discussed the posterior circulation in moyamoya disease (*12*), and no SPECT study has yet evaluated the effect of the posterior circulation on the CBF of moyamoya patients. Therefore, we reviewed the SPECT images in patients with moyamoya disease and evaluated the relationship between the anterior and the posterior circulation. We then compared these findings with parenchymal lesions detected by MRI.

MATERIALS AND METHODS

Patients

Over the past 2 yr, six consecutive patients with angiographically idiopathic moyamoya disease were studied. Three of these patients were male and three were female (age range from 10 to 54 yr; mean age 26 ± 16 [s.d.] yr). All six patients were found to have no underlying disease, thereby confirming the diagnosis of idiopathic moyamoya disease, and none had undergone previous surgical treatment.

Imaging Examinations

SPECT imaging was performed with a rotating, single-head gamma camera equipped with a low-energy, all-purpose, parallel-hole collimator. Five minutes after intravenous injection of 555–740 MBq ^{99m}Tc-HMPAO, SPECT imaging was initiated. Sixty-four views were obtained through a 360° rotation with an acquisition time of 30 sec per view, which resulted in a matrix size of 64 × 64. The camera was connected to a nuclear medicine computer. Furthermore, a Butterworth filter was applied before reconstruction and transaxial sections (a section thickness of one pixel size, 4.8 mm) were reconstructed with a standard back projection using a Shepp and Logan filter. No attenuation correction was made.

Within 1 mo after SPECT imaging, all six patients underwent MRI that was performed with a 1.5-T system using a circularly polarized quadrature head coil. Axial and coronal T1-weighted, spin-echo images were obtained with a 600/20 sequence (repetition time msec/echo time msec) and two signals averaged. Axial proton-density and T2-weighted images were obtained as the first and second echo images of the spin echo 3000/20, 80 sequence with one signal averaged, respectively. All images were acquired with a 20-cm field of view, 256 × 256 matrix and a section thickness of 5 mm with a 1-mm intersection gap.

Furthermore, using the transfemoral catheterization technique, all six patients underwent cerebral angiography that included bilateral internal external carotid arteriography and unilateral or bilateral vertebral arteriography, which was performed within 1 mo of the SPECT and MRI.

Image Analysis

On the basis of the angiographic findings, we classified steno-occlusive lesions of the internal carotid artery bifurcation, according to the degree of narrowing noted in the supraclinoid portion of the internal carotid artery and the proximal portions of the anterior cerebral artery and middle cerebral artery, into one of the five after stages: stage 1 = mild-to-moderate stenosis of the internal carotid artery bifurcation (≤80% reduction in diameter); stage 2 = severe stenosis of the internal carotid artery bifurcation (>80% reduction in diameter); stage 3 = occlusion of either the anterior cerebral artery or middle cerebral artery; stage 4 = occlusion of the internal carotid artery bifurcation, with partial retention of the anterior cerebral artery and/or middle cerebral artery main trunk; and stage 5 = occlusion of the internal carotid artery bifurcation, with no visualized anterior cerebral artery and middle cerebral artery main trunk (*13,14*). Lesions in the posterior cerebral artery (PCA) were graded as normal, stenotic or occluded.

We also classified basal cerebral moyamoya vessels (MMVs) on the basis of their presence and appearance into four grades: none, slight, moderate or marked. Marked implies that the MMVs were a vascular network that had stained heavily and extended above the basal ganglia with visualization of the medullary arteries; moderate means that the MMVs presented an intermediate vascular network localized in the basal ganglia without visualization of the medullary arteries; and slight indicates that MMVs were less dense and showed a more orderly arrangement only near the internal carotid bifurcation, assuming the appearance of unusually dilated perforating arteries.

SPECT images were reviewed for the distribution of areas showing decreased regional CBF (rCBF). Rectangular regions of interest (ROIs) were thus set on SPECT images in the frontal, temporal, parietal and occipital lobes and in the basal ganglia and cerebellar hemispheres. The size of each ROI was 20 × 20 mm, and the mean value of three or four ROIs was calculated in five regions (frontal, temporal, parietal and occipital lobes and basal ganglia). The cerebral-to-cerebellar activity ratio (C/C ratio) was calculated by dividing the count in these regions by that in the cerebellar hemisphere to assess the rCBF. Values were expressed in percentages as a mean ± s.d. of the C/C ratios.

In this regard, based on the vertebral arteriography, we confirmed that there was no abnormality in the superior cerebellar, anterior inferior cerebellar, posterior inferior cerebellar, vertebral and basilar arteries in the six moyamoya patients studied. We also included 12 normal volunteers (6 males, 6 females; aged 11 to 34 yr) as a control group in this study and found no significant difference in the number of counts in the cerebellar hemisphere between moyamoya patients (51.4 ± 2.4) and normal volunteers (52.9 ± 3.1). Thus, we believe that the cerebellar blood flow in moyamoya patients is within normal range and can serve as a reliable reference.

MR images were reviewed for a cerebral infarction and hemorrhagic lesions. On MRI, an infarction was the diagnosis for lesions that showed an abnormal signal intensity on both T1- and T2-weighted images, whereas lesions that presented an abnormal signal intensity in the deep white matter only on T2-weighted images were not included in the diagnosis of an infarction.

Imaging studies were evaluated on the basis of blinded separate interpretations by two independent radiologists. Further, SPECT and MR images were interpreted independently without knowledge of the angiographic findings. In instances when the observers did not fully agree, diagnosis was achieved by consensus.

Finally, statistical analysis was performed by using the chi-squares test, Fisher exact test, Mann-Whitney test or Spearman rank correlation test between groups, and values of $p < 0.05$ were considered as being statistically significant.

RESULTS

Steno-Occlusive Lesions and the rCBF

In all six patients, stenosis or occlusion of the supraclinoid portion of the internal carotid artery and of the proximal portions of the anterior cerebral artery and middle cerebral

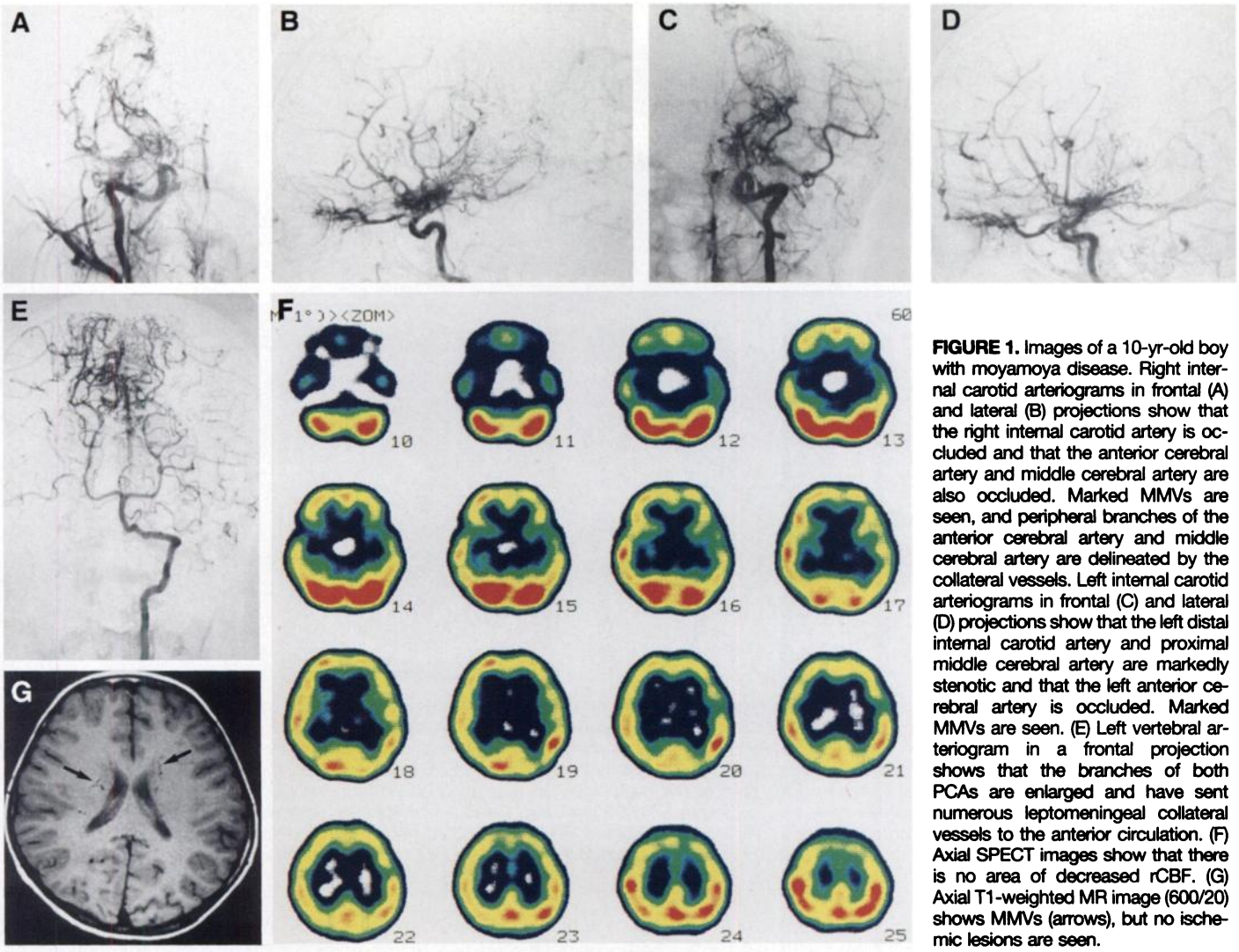

FIGURE 1. Images of a 10-yr-old boy with moyamoya disease. Right internal carotid arteriograms in frontal (A) and lateral (B) projections show that the right internal carotid artery is occluded and that the anterior cerebral artery and middle cerebral artery are also occluded. Marked MMVs are seen, and peripheral branches of the anterior cerebral artery and middle cerebral artery are delineated by the collateral vessels. Left internal carotid arteriograms in frontal (C) and lateral (D) projections show that the left distal internal carotid artery and proximal middle cerebral artery are markedly stenotic and that the left anterior cerebral artery is occluded. Marked MMVs are seen. (E) Left vertebral arteriogram in a frontal projection shows that the branches of both PCAs are enlarged and have sent numerous leptomeningeal collateral vessels to the anterior circulation. (F) Axial SPECT images show that there is no area of decreased rCBF. (G) Axial T1-weighted MR image (600/20) shows MMVs (arrows), but no ischemic lesions are seen.

artery was detected bilaterally (Figs. 1 and 2). The stages of these steno-occlusive lesions in the 12 internal carotid artery bifurcations were as follows: stage 2, two arteries; stage 3, four arteries; stage 4, four arteries; and stage 5, two arteries. Further, out of 12 PCAs, three arteries were found to be stenotic and four arteries occluded (Fig. 2). Thus, a total of seven PCAs (58%) manifested steno-occlusive lesions.

As shown in Table 1, the rCBF in the frontal, temporal, parietal and occipital lobes and the basal ganglia significantly decreased as the degree of steno-occlusive lesions of the PCA advanced ($p < 0.05$, $p < 0.01$, $p < 0.01$, $p < 0.05$ and $p < 0.05$, respectively) (Figs. 1 and 2). Thus, the presence of steno-occlusive PCA lesions was found to be greatly linked to the rCBF in moyamoya patients. On SPECT imaging, however, the stage of steno-occlusive lesions of the internal carotid artery bifurcation did not correlate significantly with the rCBF (Table 2).

Collateral Vessels and the rCBF

In all six patients, basal cerebral MMVs were detected bilaterally in the cerebral hemispheres (Figs. 1 and 2). The grade of the MMVs in 12 cerebral hemispheres was as follows: slight, five hemispheres; moderate, three hemispheres; and marked, four hemispheres. Further, leptomeningeal collateral vessels from the PCA to the anterior circulation were noted in eight cerebral hemispheres (67%) (Fig. 1), but in hemispheres that manifested occlusion of the PCA, no leptomeningeal collateral vessels from the PCA to the anterior circulation were seen (Fig. 2).

As shown in Table 3, the rCBF in the temporal, parietal and occipital lobes was significantly higher when leptomeningeal collateral vessels were present in contrast to when they were not ($p < 0.05$, $p < 0.001$ and $p < 0.01$, respectively) (Figs. 1 and 2). Further, the rCBF in the frontal lobe and basal ganglia was also higher when leptomeningeal collateral vessels were present, but not significantly. Thus, the presence of leptomeningeal collateral vessels was found to be closely linked to the rCBF. On SPECT imaging, however, the grade of basal cerebral MMVs did not significantly correlate with rCBF (Table 4).

Cerebral Infarctions on MR Images

Out of 12 cerebral hemispheres, cerebral infarctions were found in five hemispheres (42%) (Fig. 2). Further, a cerebral hemorrhage was also identified in one hemisphere (8%).

As shown in Table 5, the frequency of a cerebral infarction significantly increased as the degree of the PCA steno-occlusive lesions advanced ($p < 0.01$) (Figs. 1 and 2). Thus, the presence of steno-occlusive PCA lesions appears to be greatly linked to the occurrence of a cerebral infarction in moyamoya patients. It also should be pointed out that the stage of steno-occlusive lesions of the internal carotid artery bifurcation did not significantly correlate with cerebral infarction.

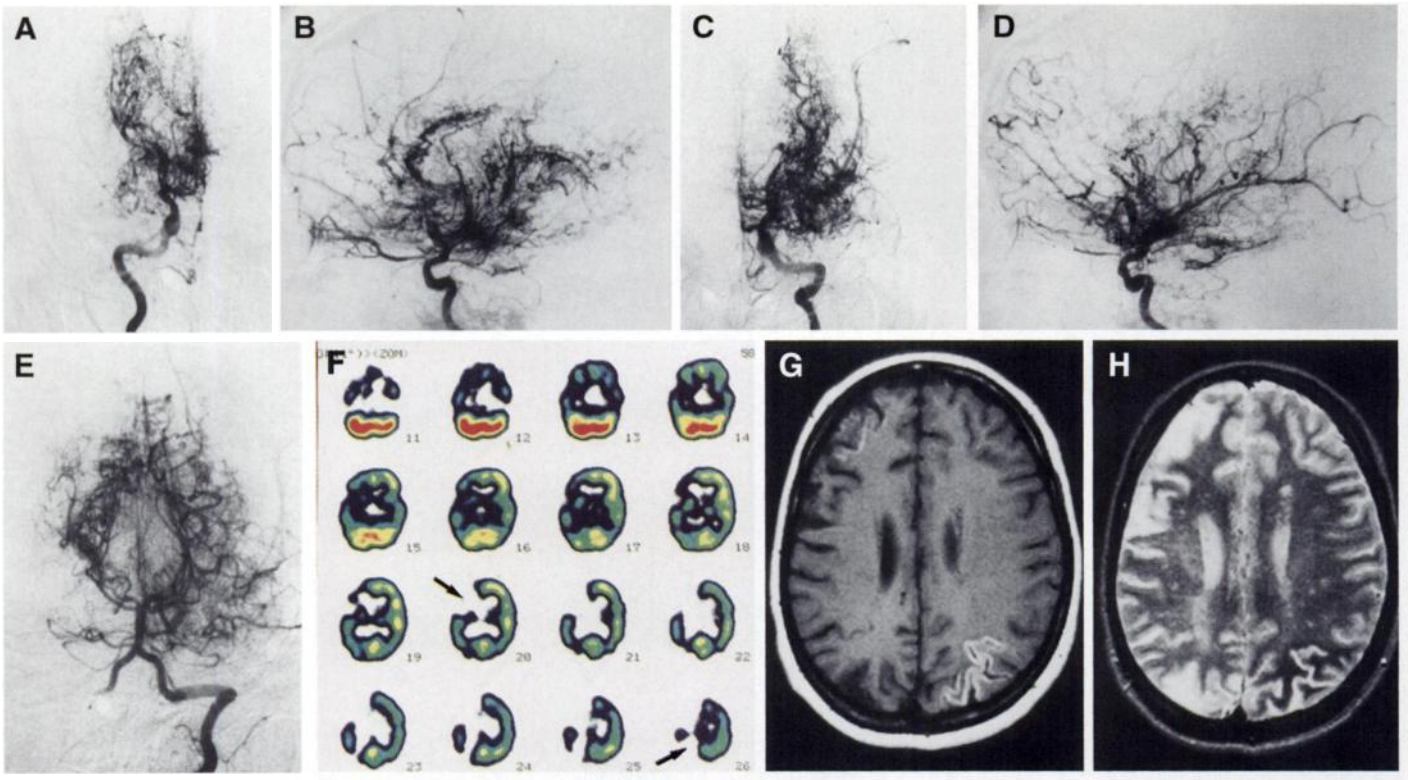

FIGURE 2. Images of an 18-yr-old woman with moyamoya disease. Right internal carotid arteriograms in frontal (A) and lateral (B) projections show that the right distal internal carotid artery and proximal anterior cerebral artery are stenotic and that the right middle cerebral artery is occluded. Marked MMVs are seen. Left internal carotid arteriograms in frontal (C) and lateral (D) projections show that the left distal internal carotid artery and proximal anterior cerebral artery are stenotic and that the left middle cerebral artery is occluded. Marked MMVs are seen. (E) Left vertebral arteriogram in a frontal projection shows that the right PCA is occluded and that the left PCA is markedly stenotic. Although MMVs are seen, there are no leptomeningeal collateral vessels to the anterior circulation. (F) Axial SPECT images show extensive areas of decreased rCBF in bilateral cerebral hemispheres. Particularly, large perfusion defect areas (arrows) are noted in the right frontal and parietal lobes. (G) Axial T1-weighted MR image (600/20) shows extensive infarctions, including hemorrhagic infarctions, in the right frontal and bilateral parietal lobes. (H) Axial T2-weighted MR image (3,000/80) shows extensive infarctions in the right frontal and bilateral parietal lobes.

DISCUSSION

In our six moyamoya patients, 7 of 12 PCAs (58%) had steno-occlusive lesions. The rCBF (C/C ratio) in all five regions of the cerebral hemisphere significantly decreased as the degree of the PCA steno-occlusive lesions advanced. Thus, the presence of steno-occlusive PCA lesions appears to be significantly linked to decreased CBF of moyamoya disease patients. No significant correlation, however, was found between steno-occlusive lesions of the internal carotid artery bifurcation and CBF. These data indicate that cerebral ischemia in moyamoya patients increases proportionally with the presence of steno-occlusive lesions of the posterior circulation rather than with steno-occlusive lesions of the anterior circulation.

The presence or absence of leptomeningeal collateral vessels from the PCA to the anterior circulation closely correlated with rCBF in the cerebral hemisphere. In moyamoya disease patients with occlusion in both internal carotid artery bifurcations, leptomeningeal collateral vessels become a major provider of compensatory cerebral blood supply (*15,16*), so that any de-

TABLE 1
PCA Lesion Grade and rCBF on SPECT Images

Region	PCA Lesion Grade			p value
	Normal (n = 5)	Stenotic (n = 3)	Occluded (n = 4)	
Frontal (n = 12)	81 ± 5	71 ± 20	65 ± 14	<0.05
Temporal (n = 12)	90 ± 9	83 ± 4	73 ± 8	<0.01
Parietal (n = 12)	92 ± 6	89 ± 4	72 ± 8	<0.01
Occipital (n = 12)	103 ± 7	95 ± 16	66 ± 25	<0.05
Basal ganglia (n = 12)	79 ± 7	71 ± 2	67 ± 8	<0.05
Total	89 ± 11	82 ± 14	69 ± 13	<0.0001

PCA = posterior cerebral artery.

TABLE 2
Stage of ICA Bifurcation Steno-Occlusive Lesion and rCBF on SPECT Images

Region	Stage of ICA Bifurcation Lesion				p value
	2 (n = 2)	3 (n = 4)	4 (n = 4)	5 (n = 2)	
Frontal (n = 12)	80 ± 5	70 ± 18	78 ± 8	61 ± 18	ns
Temporal (n = 12)	81 ± 13	78 ± 12	87 ± 11	84 ± 3	ns
Parietal (n = 12)	85 ± 15	81 ± 15	87 ± 9	85 ± 4	ns
Occipital (n = 12)	86 ± 15	94 ± 18	81 ± 37	95 ± 1	ns
Basal ganglia (n = 12)	77 ± 16	70 ± 11	74 ± 4	74 ± 3	ns
Total	82 ± 11	79 ± 16	81 ± 17	80 ± 14	ns

ns = not significant; ICA = internal carotid artery.

TABLE 3
Leptomeningeal Collateral Vessels from the PCA to the Anterior Circulation and rCBF on SPECT Images

Region	Leptomeningeal Collateral Vessels: Absence (n = 4)	Leptomeningeal Collateral Vessels: Presence (n = 8)	p value
Frontal (n = 12)	65 ± 14	77 ± 13	ns
Temporal (n = 12)	73 ± 8	87 ± 8	<0.05
Parietal (n = 12)	72 ± 8	90 ± 5	<0.001
Occipital (n = 12)	66 ± 25	100 ± 11	<0.01
Basal ganglia (n = 12)	67 ± 8	76 ± 7	ns
Total	69 ± 13	86 ± 12	<0.0001

ns = not significant; PCA = posterior cerebral artery.

crease in the leptomeningeal collateral vessels would critically influence CBF. The subsequent decrease in the leptomeningeal collateral vessels is due to progressive steno-occlusive lesions of the PCA, and when the PCA finally becomes occluded, leptomeningeal collateral vessels, which supply compensatory blood flow to the ischemic brain, disappear, thereby resulting in severe cerebral ischemia.

In contrast, the grade of the basal cerebral MMVs in moyamoya patients did not correlate with the rCBF, and though the presence of basal cerebral MMVs is the most characteristic finding in moyamoya disease (*1,2*), the contribution of the basal cerebral MMVs to CBF appears to be far lower than that of leptomeningeal collateral vessels.

As for MRI results, the frequency of cerebral infarction significantly increased as the degree of steno-occlusive lesions of the PCA advanced. Thus, the presence of steno-occlusive PCA lesions appears to be significantly linked to the occurrence of cerebral infarctions in moyamoya disease patients. As was noted previously, no significant correlation was found between steno-occlusive lesions of the internal carotid artery bifurcation and a cerebral infarction.

TABLE 4
Basal Cerebral MMVs and rCBF on SPECT Images

Region	Basal Cerebral MMVs: Slight (n = 5)	Moderate (n = 3)	Marked (n = 4)	p value
Frontal (n = 12)	73 ± 14	81 ± 5	67 ± 17	ns
Temporal (n = 12)	87 ± 12	83 ± 7	77 ± 10	ns
Parietal (n = 12)	87 ± 9	90 ± 6	77 ± 13	ns
Occipital (n = 12)	93 ± 10	99 ± 18	75 ± 34	ns
Basal ganglia (n = 12)	75 ± 8	75 ± 9	69 ± 9	ns
Total	83 ± 13	86 ± 12	73 ± 17	ns

ns = not significant; MMVs = moyamoya vessels.

TABLE 5
Angiographic Findings and Cerebral Infarction on MR Images

Angiographic findings	Cerebral Infarction: Absence (n = 7)	Cerebral Infarction: Presence (n = 5)	p value
PCA lesion			
Normal (n = 5)	5	0	
Stenotic (n = 3)	2	1	<0.01
Occluded (n = 4)	0	4	
Stage of ICA bifurcation			
2 (n = 2)	2	0	
3 (n = 4)	2	2	ns
4 (n = 4)	2	2	
5 (n = 2)	1	1	

ns = not significant; PCA = posterior cerebral artery; ICA = internal carotid artery.

CONCLUSION

The rCBF in moyamoya patients decreases proportionally based on the degree of steno-occlusive lesions of the PCA. Therefore, if the degree of steno-occlusive PCA lesions is great, a decrease occurs in the leptomeningeal collateral vessels to the anterior circulation, thereby causing severe cerebral ischemia that is likely to result in an infarction.

REFERENCES

1. Nishimoto A, Takeuchi S. Abnormal cerebrovascular network related to the internal carotid arteries. *J Neurosurg* 1968;29:255–260.
2. Suzuki J, Takaku A. Cerebrovascular "moyamoya" disease: disease showing abnormal net-like vessels in base of brain. *Arch Neurol* 1969;20:288–299.
3. Taveras JM. Multiple progressive intracranial arterial occlusions: a syndrome of children and young adults. *Am J Roentgenol* 1969;106:235–268.
4. Pecker J, Simon J, Guy G, Herry JF. Nishimoto's disease: significance of its angiographic appearances. *Neuroradiology* 1973;5:223–230.
5. Handa J, Handa H. Progressive cerebral arterial occlusive disease: analysis of 27 cases. *Neuroradiology* 1972;3:119–133.
6. Takahashi M. Magnification angiography in moyamoya disease: new observations on collateral vessels. *Radiology* 1980;136:379–386.
7. Hasuo K, Tamura S, Kudo S, et al. Moyamoya disease: use of digital subtraction angiography in its diagnosis. *Radiology* 1985;157:107–111.
8. Mountz JM, Foster NL, Ackermann RJ, Bluemlein L, Petry NA, Kuhl DE. SPECT imaging of moyamoya disease using ^{99m}Tc-HMPAO: comparison with computed tomography findings. *J Comput Tomogr* 1988;12:247–250.
9. Ohashi K, Fernandez-Ulloa M, Hall LC. SPECT, magnetic resonance and angiographic features in a moyamoya patient before and after external-to-internal carotid artery bypass. *J Nucl Med* 1992;33:1692–1695.
10. Inoue Y, Momose T, Machida K, Honda N, Tsutsumi K. Cerebral vasodilatory capacity mapping using technetium-99m-DTPA-HSA SPECT and acetazolamide in moyamoya disease. *J Nucl Med* 1993;34:1984–1986.
11. Hoshi H, Ohnishi T, Jinnouchi S, et al. Cerebral blood flow study in patients with moyamoya disease evaluated by IMP SPECT. *J Nucl Med* 1994;35:44–50.
12. Miyamoto S, Kikuchi H, Karasawa J, Nagata I, Ikota T, Takeuchi S. Study of the posterior circulation in moyamoya disease: clinical and neuroradiological evaluation. *J Neurosurg* 1984;61:1032–1037.
13. Satoh S, Shibuya H, Matsushima Y, Suzuki S. Analysis of the angiographic findings in cases of childhood moyamoya disease. *Neuroradiology* 1988;30:111–119.
14. Yamada I, Matsushima Y, Suzuki S. Moyamoya disease: diagnosis with three-dimensional time-of-flight MR angiography. *Radiology* 1992;184:773–778.
15. Takeuchi S, Tanaka R, Ishii R, Tsuchida T, Kobayashi K, Arai H. Cerebral hemodynamics in patients with moyamoya disease: a study of regional cerebral blood flow by the ^{133}Xe inhalation method. *Surg Neurol* 1985;23:468–474.
16. Yamada I, Matsushima Y, Suzuki S. Childhood moyamoya disease before and after encephalo-duro-arterio-synangiosis: an angiographic study. *Neuroradiology* 1992;34:318–322.